Design of Reconfigurable Antenna Feeding Network Using Coupled-line Switch for 5G Millimeter-wave Communication System

Sangkil Kim [1] and Jusung Kim [2*]

[1] Department of Electronics Engineering
Pusan National University, Busan, 46241, South Korea
ksangkil3@pusan.ac.kr

[2] Department of Electronics and Control Engineering
Hanbat National University, Daejeon, 34158, South Korea
jusungkim@hanbat.ac.kr*

Abstract ─ In this paper, a reconfigurable antenna feeding network using coupled line switches for 5G communication system is presented. Two quarter-wave impedance transformers were integrated to support TDD operation and a single stage coupled line filter was used as a DC block for RF switches instead of using conventional surface mounting components. Design equations and theoretical analysis for the proposed reconfigurable antenna feeding network are also presented. To demonstrate the performance of the proposed reconfigurable antenna feeding system for MIMO, two monopole antennas were integrated orthogonally to the designed feeding network. Vertical or horizontal polarization was successfully formed and the radiation pattern can be selectable by manipulating the switches.

Index Terms ─ 5G communication system, coupled line switch, MIMO antenna, mmWave antenna, reconfigurable antenna feeding network, System-on-Package (SoP) technology.

I. INTRODUCTION

The millimeter wave (mmWave) communication system is promising technology for 5G communication. The 5G mmWave communication technology has received great attention from many researchers and industry, and there has been a lot of reported research efforts on mmWave-based 5G communication system [1-3]. It is possible to achieve high network throughput and data rate as high as gigabits per second (Gbps) by leveraging massive multiple-input multiple-output (MIMO) technology. It can also handle over thousand times more mobile traffic than previous mobile communication networks such as 4G LTE [2]. It is reported that time-division duplex (TDD) is more efficient in a wireless backhaul network that uses massive MIMO in small cells compared to frequency-division duplex (FDD) [3]. Since TDD can handle asymmetric data rates in the uplink and downlink, TDD does not require the same frequency spectrum as FDD. Therefore, TDD provides more flexibility in 5G communication (Tx/Rx). It can also dynamically allocate channel capacity based on the communication traffic load. In the case of massive MIMO, the 5G communication system also requires an array antenna with dual polarization capability.

In this paper, a polarization and radiation pattern reconfigurable antenna feeding network consisting of coupled line switches and quarter-wave impedance transformers is presented. This paper also provides a computational design and modeling idea for 5G mmWave module designs consisting of an RFIC and an antenna array. Two quarter-wave impedance transformers are integrated to support TDD operation and reduces the number of antennas for system miniaturization. The uplink (Tx) and downlink (Rx) paths are successfully isolated by the designed quarter-wave impedance transformer. A coupled line-based PIN diode switch is proposed to decouple the DC bias path from RF signal path because there are not many available SMD passive components such as inductors or capacitors working in the frequency band above 28 GHz. Two monopole antennas were placed orthogonally through the coupled line RF switch to reconstruct the antenna polarization and radiation pattern for MIMO applications. The proposed reconfigurable antenna feeding network can be easily extended to a large array system, but a single Tx/Rx pair is discussed in this paper as a proof-of-concept without loss of generality.

This paper is organized as follows. Section II discusses the design of the proposed reconfigurable antenna feeding network for mmWave applications using coupled line switches. Section III shows the system performance by integrating two monopole antennas with the reconfigurable feeding network shown in Section II.

Submitted On: May 2, 2018
Accepted On: July 22, 2018

It is followed by conclusion.

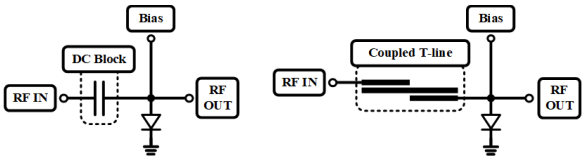

(a) (b)

Fig. 1. (a) A conventional SPST switch, and (b) the proposed coupled line switch for mmWave applications.

II. RECONFIGURABLE ANTENNA FEEDING NETWORK

It is important to select proper fabrication technology for a design because fabrication resolution (metal-to-metal distance, metal width/thickness, *etc.*) and electrical material properties (ε_r, and tan δ) are critical design parameters for design feasibility and system implementation.System-on-Package (SoP) technology using flip chip ball grid array (FCBGA) packaging has been chosen because it offers fine feature sizes up to 20 μm and is widely used in RFIC industry for high system integrity and multi-die handling capability [4]. A 15 μm thick copper layer is deposited on a 40 μm thick substrate material which has dielectric constant (ε_r) of 3.4 and loss tangent (tan δ) of 0.0044 at 28 GHz [5]. The microstrip line structure was chosen in the system design because it is easy to implement the design and it is enough to show the proof-of-concept presented in this paper. It has been proved with many reported research efforts that the microstrip and strip line structures can be fabricated with high reliability along with good correlation between simulation and measurement results [6,7].

A. Ports and lumped elements models

It is important to set the ports appropriately and build lumped elements models for the accuracy of the simulation results. A voltage or a current source is a good excitation model that describes voltage or current flow from the IC. Therefore, bumps of IC chip should be excited by a lumped port model. Other ports for the transmission lines should be excited by a waveguide port to excite the quasi-TEM mode of the microstrip line.

The PIN diode switch can be modeled as a series or a parallel RLC tank when it is turned 'on' or 'off'. It has low resistance when the diode switch is on, and it has high resistance when the switch is off. For the Finite Element Method (FEM), the lumped element can be modeled as a 2D rectangular sheet (width: *w*, length: *l*) having tangential E and H fields (E_t, H_t) for the sheet. The lumped impedance (Z_l) is described by voltage (V) and current (I) as $Z_l = V/I$. The current, I, flows in the length-direction and the voltage difference, V, is measured between the two terminals along the length. The field impedance (Z_f) is also described by the tangential field components as $Z_f = E_t/H_t$. Z_l and Z_f can be related by the definition of $V = \int E_t dl = E_t \cdot l$ and $I = \oint_c H_t dc = H_t \cdot w$ where c is a closed contour surrounding the sheet. Therefore, the Z_l and Z_f can be described as $Z_f = \left(\frac{w}{l}\right) Z_l$.

There are many important issues with building accurate EM model in mmWave. Those are parasitic coupling, passive/active component models, signal dispersion and loss of transmission line [8]. Three-dimensional full wave FEM analysis was chosen to capture all the possible couplings and radiations in the proposed circuit in this paper. The nonlinear diode switch was modeled as a parallel passive RC tank depending on its state as discussed. Surface roughness and metal thickness were also considered for better modeling of the mmWave SoP technology.

B. Coupled line switch for mmWave applications

Figure 1 (a) shows a simplified conventional single-pole single-throw (SPST) RF switch. It consists of a single PIN diode and a DC bias circuit. A DC block capacitor is an important component of the switch operation to decouple the RF signal from the DC bias of the PIN diode. A high capacitance value (nF ~ μF or higher) with sufficient quality factor (Q) in the GHz frequency band is desirable because it provides low RF impedance (almost short circuit) while isolating the RF path from the DC bias circuit. Surface-mount devices (SMDs) are widely used as DC block capacitors since they are small enough to be considered lump components (< $\lambda_0/20$) in the frequency band below 10 GHz. However, it is challenging to use lumped SMDs for mmWave applications operating at 28 GHz or higher. It is due to the low self-resonant frequency (SRF) of the SMDs, high parasitic values, and the large size of the components compared to the wavelength at 28 GHz.

Figure 1 (b) shows the proposed coupled microstrip line switch for mmWave applications. The coupled microstrip line separates the DC bias path from RF signal path, and suppresses even harmonics from RF circuit (RF_{IN}). The proposed design does not require SMDs for the DC block and the coupled line can be designed to achieve better harmonic rejection or the desired phase shift.

C. Quarter-wave transformer section

Two quarter-wave ($\lambda/4$) impedance transformers are designed to transform the output (input) impedance of PA (LNA) as shown in Fig. 2. For instance, the PA output pin is connected to the $\lambda/4$ transformer at pin ① and the transformer at pin ② is connected to ground at Tx mode. Theoretically, the load impedance of the $\lambda/4$ transformer

at pin ① is the output impedance of PA (Z_{L1}) when the impedance at pin ② is 0 Ω (Z_{L2}). The impedance seen looking into the pin ③ ($Z_{in,\lambda/4}$) can be expressed as (1):

$$Z_{in,\lambda/4} = \left[Z_1 \frac{Z_{L1}+jZ_1\tan(\beta\cdot l_{Q1})}{Z_1+jZ_{L1}\tan(\beta\cdot l_{Q1})}\right] || \left[Z_2 \frac{Z_{L2}+jZ_2\tan(\beta\cdot l_{Q2})}{Z_2+jZ_{L2}\tan(\beta\cdot l_{Q2})}\right], \quad (1)$$

where β is a propagation constant. Z_1 and l_{Q1} are the characteristic impedance and length of the $\lambda/4$ transformer at ①-③ while Z_2 and l_{Q2} are those of the transformer at ②-③. Since $\beta \cdot l_{Q1} = \beta \cdot l_{Q2} = \pi/2$ for a quarter-wave transmission line, $Z_{in,\lambda/4}$ can be simplified as (2) when $Z_1 = Z_{L1}$ (matched case):

$$Z_{in,\lambda/4} = Z_{L1} || \infty = Z_{L1}. \quad (2)$$

Therefore, the impedance seen looking into a bump (①: Tx, Z_{L1} or ②: Rx, Z_{L2}) shows up at pin ③ ($Z_{in,\lambda/4}$) without loading each other due to the impedance transformation. An antenna can be shared with the Tx and Rx modes due to the quarter-wave impedance transformer, which reduces the number of required antennas.

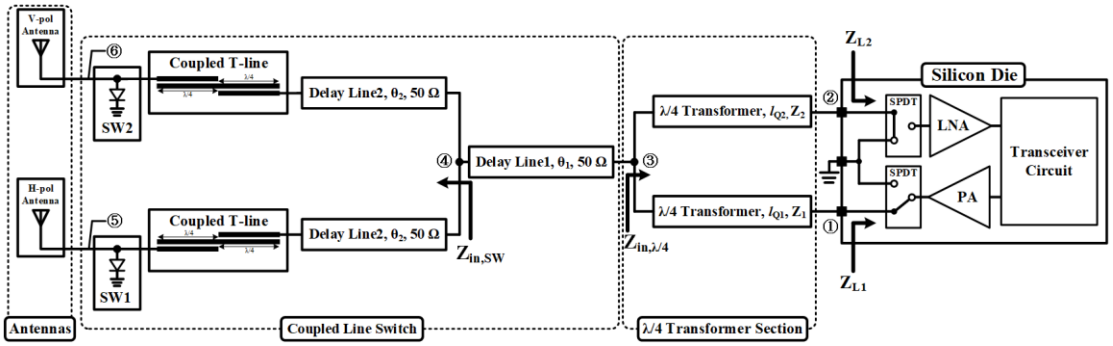

Fig. 2. Block diagram of the proposed reconfigurable antenna feeding network for 5G mmWave communication system.

Figure 3 shows the S-parameters of a quarter-wave transformer using a microstrip line structure. The distance between Tx/Rx bumps is 300 μm. In this design, the quarter-wave length (l_{Q1}, l_{Q2}) at 28 GHz is about 1700 μm, and the width of the 50 Ω microstrip line is about 81 μm according to the design equations reported in [9]. The insertion loss (IL) of the designed quarter-wave transformer section is about 0.25 dB, and it has broad fractional bandwidth of 70.1% (17.08 GHz ~ 36.71 GHz) at 28 GHz. The bandwidth is wide enough to cover 5G communication frequency band of 26.65 GHz ~ 29.19 GHz used in Korea and North America. It also provides a good isolation level of 35 dB between the Tx and Rx paths at the operation frequency

D. Coupled line impedance transformer and switch

The parallel coupled microstrip line is a critical part of the proposed system because it separates the DC bias circuit from RF signal path. It also suppresses even harmonics from a non-linear circuit since it follows coupled T-line bandpass filter theory. The single branch of the coupled line switch shown in Fig. 2 consists of a coupled line impedance transformer and a PIN diode switch. The coupled line impedance transformer can be modeled as a single stage (N=1) coupled line filter having a delay line as shown in Fig. 4. The coupling effect between the two parallel microstrip lines is modeled as admittance inverter, $\boldsymbol{J}$, because of the capacitive coupling [10]. The electrical length of the coupled lines (θ_3) is set to 90° (π/2) at the center frequency of the passband (28 GHz) to obtain band-pass frequency response. The delay line2 compensates the phase required to transform a low impedance to a high impedance ($Z_{in,SW}$), such as a quarter-wave impedance transformer, when the switch is turned on (short circuit) at ⑤/⑥ as shown in Fig. 4 (a). The delay line1 connects the coupled switches to the quarter-wave transformer. There is no impedance transformation through delay line1 because it is matched to the transformer and the switch section. The electrical length of delay line1 (θ_1) can be appropriately selected to achieve the desired phase delay.

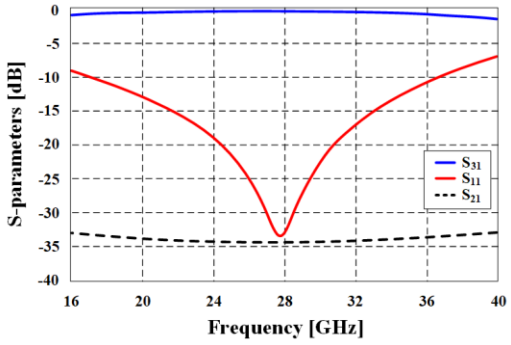

Fig. 3. S-parameters of the designed $\lambda/4$ transformer section.

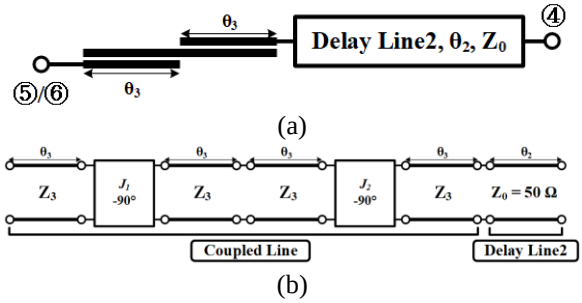

Fig. 4. (a) Proposed coupled line impedance transformer without diode switch, and (b) its equivalent transmission line model.

The design equations of the coupled microstrip line is written as (3) ~ (5) according to the coupled line band-pass filter theory when the length of the coupled line is quarter-wavelength ($\theta_3 = \pi/2$) [11]. The transformed impedance ($Z_3\boldsymbol{J}_1$ and $Z_3\boldsymbol{J}_2$) can be calculated as (3) and (4) where Δ is a fractional bandwidth and g_1/g_2 are element values for maximally flat lowpass filter prototypes:

$$Z_3\boldsymbol{J}_1 = \sqrt{\frac{\pi\Delta}{2g_1}}, \tag{3}$$

$$Z_3\boldsymbol{J}_2 = \sqrt{\frac{\pi\Delta}{2g_1g_2}}. \tag{4}$$

The even (Z_{3e}) and odd mode (Z_{3o}) impedances can be extracted from (5) using characteristic impedance (Z_3) of the transmission line:

$$\begin{cases} Z_{3e} = Z_3 \cdot (1 + \boldsymbol{J}Z_3 + (\boldsymbol{J}Z_3)^2) \\ Z_{3o} = Z_3 \cdot (1 - \boldsymbol{J}Z_3 + (\boldsymbol{J}Z_3)^2) \end{cases}. \tag{5}$$

For simplicity and symmetry of design, $g_1 = g_2 = 2$ and $Z_3 = 50\ \Omega$ were chosen as the initial values. The fractional bandwidth, Δ, was set to 0.7 which has the same bandwidth as the quarter-wave transformer presented in the previous section. The calculated initial Z_{3e} and Z_{3o} were 114.56 Ω and 40.42 Ω, respectively. It requires 22.8 μm width and 14.0 μm gap which are not practical. Generally, fabrication resolution varies by manufacturer, but for most manufacturers, a 25 μm width and a 20 μm gap are most widely accepted minimum width/gap feature sizes [5]. Final even/odd impedance values (Z_{3e}/Z_{3o}) and physical dimensions (line width/gap) are iteratively derived using the design equations starting at the initial values by adjusting the fractional bandwidth (Δ) and characteristic impedance (Z_3). The final design parameter values are: $\Delta = 0.32$, $Z_3 = 60\ \Omega$, $Z_{3e} = 105.2\ \Omega$, $Z_{3o} = 45\ \Omega$. The final line width and the gap of the coupled line were 30 μm and 20 μm, respectively.

Figure 5 shows the impedance of a single coupled line switch segment (Fig. 4) at 27.5~28.5 GHz on Smith chart when diode switch 1 is on (shorted to GND). Delay line2 successfully transforms low impedance to high impedance and requires an electrical length of about $0.19\lambda_g$ (about 1300 μm). Figure 6 shows S-parameters of the proposed single coupled line switch. The insertion loss is 0.89 dB and the 3-dB bandwidth is 8.96 GHz (fractional bandwidth: 31.7%). A DC block using a SMD capacitor for millimeter wave application is also shown in Fig. 6 for comparison purposes. The capacitance value of the SMD was 82 pF (0.07 Ω at 28 GHz), and its size was 1.4 mm × 0.5 mm (0502 SMD standard). It has an operation frequency range of up to 40 GHz [12]. The IL of the DC block utilizing SMD capacitor is 1.21 dB and it has reflection coefficient of -7.54 dB at 28 GHz. It has 0.3 dB higher loss and relatively poor reflection coefficient than the proposed coupled line-based DC block. S_{54} of the proposed RF switch network shows the band-pass response in contrast to the flat S_{54} of a conventional RF switch. Therefore, the proposed RF switch provides more immunity to out-of-band interferences.

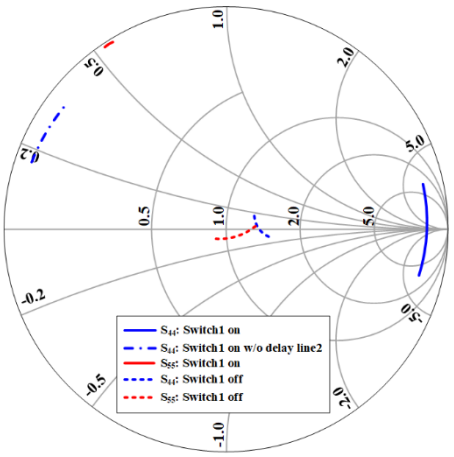

Fig. 5. Impedance of the switch: On/Off states.

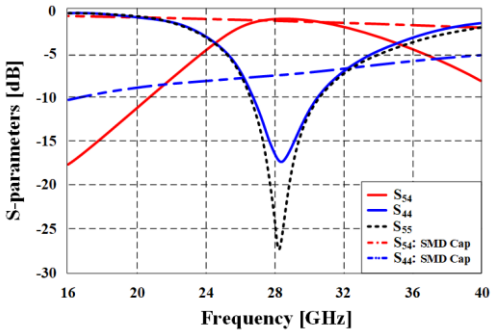

Fig. 6. S-parameters of the designed coupled line impedance transformer and a conventional DC block using SMD capacitor for mmWave applications.

E. Reconfigurable antenna feeding network

In this section, a reconfigurable antenna feeding network was constructed by integrating the designed quarter-wave impedance transformer and two coupled

line switches. The signal input pins were ① (Tx mode)/② (Rx mode) and the output pins were ⑤ (H-pol antenna)/ ⑥ (V-pol antenna) (shown in Fig. 2). The switches (SW1 and SW2) exclusively direct the signal to the desired path. For example, signal is directed to ⑥ from ① when SW1 is 'on' and SW2 is 'off' while input pin of LNA, ②, is pull-down to ground in case of Tx mode.

Figure 7 summarizes the performance of the proposed reconfigurable antenna feeding network. The total IL at 28 GHz is 1.57 dB, and 3-dB bandwidth is 25.17 GHz ~ 30.78 GHz (5.61 GHz) which is wide enough to cover the target bandwidth (26.65 GHz ~ 29.19 GHz). The total insertion loss (between ① and ⑤/ ⑥) includes the loss of $\lambda/4$ transformer (0.25 dB), coupled line switch (0.89 dB), T-junction (connecting two coupled line switches for V-/H- antennas: 0.43 dB). It should be noted that there is almost no difference between switch operation modes (SW1-on/SW2-off or SW1-off/SW2-on cases). The isolation level between antenna ports (⑤ and ⑥) is 42.59 dB. It also provides the 2nd harmonic suppression of 31.92 dB at 56 GHz. It is demonstrated that the RF signal path can be reconfigured with a high isolation level.

III. RECONFIGURABLE ANTENNA SYSTEM

All proposed designs were integrated and two monopole antennas were also placed at the output ports of the designed system to demonstrate re-configurability as shown in Fig. 8. The length of the monopole antenna (L1) is 2250 μm and its width (W3) is 60 μm. The distance between the coupled line switch and the monopole antenna (L2) is 1000 μm. The width (W2) and the length (C2) of the single segment of the coupled microstrip line is 30 μm and 1720 μm, respectively, while the gap (G1) between the coupled lines is 20 μm as shown in Fig. 8 (b). The two coupled line switches were arranged orthogonally to enable dual polarization (V- and H-polarization) capability using two linearly polarized antennas. The delay line 1 and 2 have the same width (W1) of 81 μm because they are 50 Ω transmission lines. The length of delay line1 (D1) is 925 μm, and that of delay line2 (D2) is 1305 μm. The geometry of the quarter-wave transformer is shown in Fig. 8 (c). It consists of two quarter-wave impedance transformers with a length of 1708 μm and a width of 81 μm. Fig. 8 (d) shows a design example of MIMO application using the monopole antennas. The Tx/Rx bumps of the IC chip feed each V/H branch to drive the antennas. The points from P1 to P4 are DC bias points as well as antenna feeding points. More compact module can be designed using multi-layers. Patch-type antennas can be easily integrated with the proposed feeding network on different layers by placing vias at P1 ~ P4. The hairpin type coupled line structure can further reduce the overall size of the proposed system.

The frequency responses of the proposed reconfigurable antenna system are shown in Fig. 9. The -10 dB bandwidth of each antenna mode is 26.13 GHz ~ 29.46 GHz (fractional bandwidth: 11.9%) which is wide enough to cover design goal of 26.65 GHz ~ 29.19 GHz (9.1%) for 5G communication frequency band. It should be noted that the reflection coefficient (S_{11}) values of the four antennas (Tx/Rx & H-/V-pol) are almost the same as shown in Fig. 9. The small discrepancy between the vertical polarization (V-pol) and the horizontal polarization (H-pol) mode is due to the T-junction where the delay line1 and 2 meet because it is not symmetric geometry, but it is negligible.

Figure 10 shows the normalized radiation patterns of the designed reconfigurable antenna system. The radiation patterns were changed according to the operation mode. The maximum realized gain of H-pol case was 2.54 dB and that of V-pol was 2.49 dB. E-plane of the proposed reconfigurable antenna system changed from *YZ*-plane to *XZ*-plane when the switch 1 was 'on' and switch 2 was 'off', or vice versa.

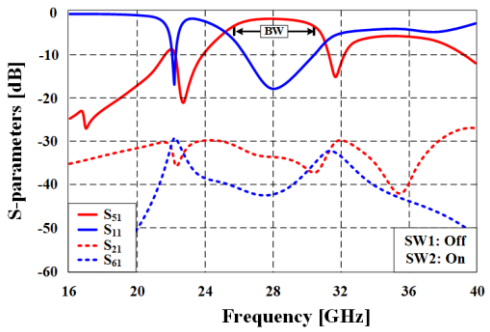

(a)

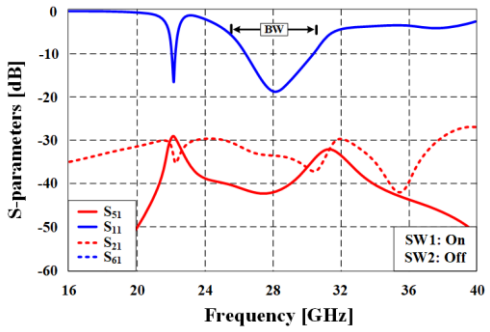

(b)

Fig. 7. S-parameters of the integrated coupled line switch and the quarter-wave transformer: (a) SW1-off/SW2-on case, and (b) SW1-on/SW2-off case.

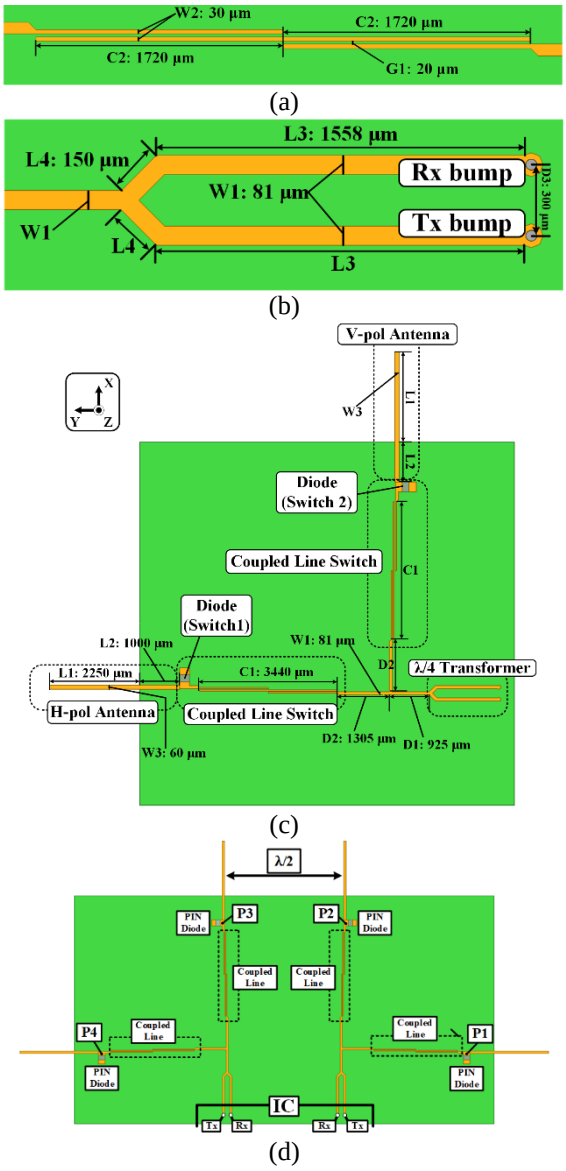

Fig. 8. System Geometry: (a) reconfigurable feeding network with dipole antennas, (b) coupled line section, (c) quarter-wave transformer section, and (d) a design example for MIMO application.

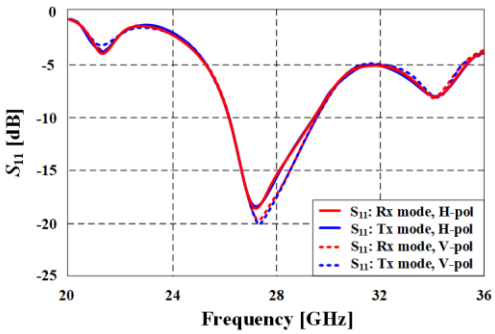

Fig. 9. S_{11} of the antenna system.

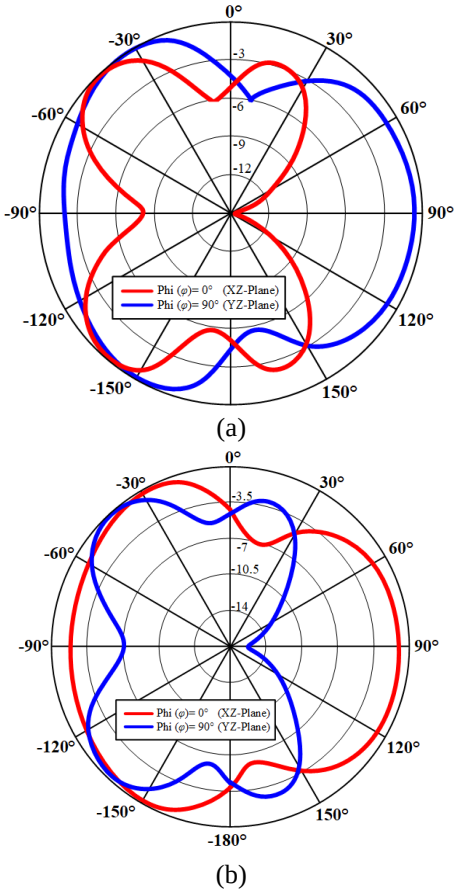

Fig. 10. Radiation patterns of the antenna system: (a) H-pol mode and (b) V-pol mode.

VI. CONCLUSION

A reconfigurable antenna feeding network using SoP technology is successfully presented in this paper. Two segments of the quarter-wave impedance transformer isolate the Tx and Rx modes by converting the low impedance of the in-active port to high

impedance. A single stage coupled microstrip line filter was proposed instead of SMD type device to separate the DC bias and RF signal path of the diode switch. The proposed switch network provides better insertion loss and suppress higher order even harmonics. The system performance was verified by integrating two monopole antennas with the re-configurable feeding network. Radiation patterns and polarization can be easily switched by manipulating the diode switches. The presented reconfigurable system is suitable for 5G communication systems and MIMO applications due to its polarization and radiation pattern re-configurability.

ACKNOWLEDGMENT

This work was supported by a 2-Year Research Grant of Pusan National University. This work was supported by the National Research Foundation of Korea

(NRF) grant funded by the Korea Government (MSIP) (No. 2016R1C1B1012042).

REFERENCES

[1] Q. Li, H. Niu, A. Papathanassiou, and G. Wu, "5G network capacity: Key elements and technologies," *IEEE Veh. Technol. Mag.*, vol. 9, no. 1, pp. 71-78, Mar. 2014.

[2] O. Elijah, C. Y. Leow, T. A. Rahman, S. Nunoo, and S. Z. Iliya, "A comprehensive survey of pilot contamination in massive MIMO–5G system," *Commun. Surveys Tuts.*, vol. 18, no. 2, pp. 905-923, 2016.

[3] Z. Gao, L. Dai, D. Mi, Z. Wang, M. A. Imran, and M. Z. Shakir, "MmWave massive-MIMO-based wireless backhaul for the 5G ultra-dense network," *IEEE Wirel. Commun.*, vol. 22, no. 5, pp. 13-21, Oct. 2015.

[4] K. Lim, S. Pinel, M. Davis, A. Sutono, C. Lee, D. Heo, A. Obatoynbo, J. Laskar, M. Tentzeris, and R. Tummala, "RF-system-on-package (SoP) for wireless communications," *IEEE Microw. Mag.*, vol. 3, no. 1, pp. 88-99, Mar. 2002.

[5] [Online] http://www.statschippac.com/documentlibrary/fcBGA.pdf

[6] Y. Liu, L. Xia, and R. Xu, "A broadband microstrip-to-microstrip vertical via interconnection for low temperature co-fired ceramic applications," *Applied Computational Electromagnetics Society (ACES) Express Journal*, vol. 32, no. 12, Dec. 2017.

[7] T. Sarrazin, R. Crunelle, O. Lafond, M. Himdi, N. Rolland, and L. Roy, "A 60GHz aperture-coupled micromachined microstrip antenna for heterogeneous 3D integration (system-in-package)," *Proc. 27th Int. Review of Progress in Applied Computational Electromagnetics (ACES)*, Williamsburg, Virginia, USA, Mar. 2011.

[8] K. C. Gupta, "Emerging trends in millimeter-wave CAD," *IEEE Trans. Microw. Theory Tech.*, vol. 46, no. 6, pp. 747-755, June 1998.

[9] K. C. Gupta, R. Garg, and I. J. Bahl, *Microstrip Lines and Slotlines*. Artech House, Dedham, Mass., 1979.

[10] D. M. Pozar, *Microwave Engineering*. 3rd ed., Hoboken, NJ, USA: Wiley, 2005.

[11] S. B. Cohn, "Parallel-coupled transmission-line-resonator filters," *IRE Trans. Microw. Theory Tech.*, vol. 6, no. 2, pp. 223-231, Apr. 1958.

[12] [Online] http://www.knowlescapacitors.com/dilabs/en/globalnavigation/products/broadband-blocking-capacitors#Milli_Cap